



The Impact of Layers Orientation on the Mechanical Properties in the Manufacturing of 3D Printed Prosthetic Shanks

Zainab Y. Hussein¹, Ahmed K. Muhammad², Dania Atheer Abdulbaqi³, Kadhim K. Resan²,
Mohammed Ali Abdulrehman^{2*}, Ali M. Flayyih²

¹ Project and Construction Division, Mustansiriyah University, 10045 Baghdad, Iraq

² Department of Materials Engineering, College of Engineering, Mustansiriyah University, 10045 Baghdad, Iraq

³ Department of Civil Engineering, Al Hikma University College, 10015 Baghdad, Iraq

* Correspondence: Mohammed Ali Abdulrehman (mohammed.ali_mat@uomustansiriyah.edu.iq)

Received: 03-17-2026

Revised: 04-27-2026

Accepted: 05-22-2026

Citation: Z. Y. Hussein, A. K. Muhammad, D. A. Abdulbaqi, K. K. Resan, M. A. Abdulrehman, and A. M. Flayyih, "The impact of layers orientation on the mechanical properties in the manufacturing of 3D printed prosthetic shanks," *Int. J. Comput. Methods Exp. Meas.*, vol. 14, no. 2, pp. 207–218, 2026. <https://doi.org/10.56578/ijcmem140203>.



© 2026 by the author(s). Licensee Acadlore Publishing Services Limited, Hong Kong. This article can be downloaded for free, and reused and quoted with a citation of the original published version, under the CC BY 4.0 license.

Abstract: The evolution of prosthetic devices has been influenced by the advent of additive manufacturing, particularly 3D printing, to produce prosthetic devices with reduced weight and customized designs. However, the mechanical properties of 3D printed prosthetic shanks have been affected by the printing orientation, considering the anisotropic nature of the fused deposition modeling (FDM) process. This article presents the effects of layer orientation on the mechanical and fatigue properties of prosthetic components made of polylactic acid (PLA) using 3D printing and FDM. Standard tensile and fatigue test samples were prepared using PLA and printed using FDM. Three printing orientations were used to prepare the samples. The results of the tensile test showed the anisotropic nature of the printed samples, as the yield strength of the samples printed horizontally was greater (61.3 and 60.7 MPa) than that of the samples printed vertically (24.7 MPa), representing a reduction of approximately 60%. Fatigue life analysis of the samples showed that the fatigue life of the samples printed in orientations A and B was greater than that of the samples printed in orientation C, as the bonding between the filaments of the printed samples in these two orientations was greater. Analysis of the ground reaction force (GRF) showed that the highest force occurred during the toe-off phase of the gait cycle. These results were used to evaluate the structural safety of prosthetic shanks using finite element analysis (FEA). From the results, it is evident that the printing orientation significantly affects the stress and failure of the prosthetic shanks.

Keywords: Finite element analysis; Layer orientation; Prosthetic shank; 3D printing; Polylactic acid

1 Introduction

In recent years, advances in additive manufacturing technologies, specifically in 3D printing, have had an impact on the design of prostheses by allowing the creation of custom-shaped prosthetic shanks according to individual anatomy needs [1–4]. Conventionally, prosthetic limbs are made of rigid materials, which could lead to poor adaptability and comfort. Instead, 3D printing enables the manufacturing of lightweight and functionally optimized parts, thereby increasing the mobility of the wearer [5–7]. However, the mechanical performance of 3D-printed objects remains extremely sensitive to the printing parameters. Among the factors affecting the characteristics of additive manufacturing parts, there is the issue of filament orientation, which is one of the key parameters for the development of anisotropic structures, where strength, durability, and even flexibility depend on the orientation [8–10]. Therefore, knowledge of the effect of filament orientation on key properties of 3D-printed parts, such as tensile strength and fatigue resistance, is vital for achieving high-quality prosthetic devices [2, 11, 12].

It has already been proven that the mechanical performance of horizontally printed specimens is superior because of the enhanced interlayer bonding along the loading direction. Conversely, vertically printed parts tend to exhibit inferior mechanical characteristics owing to their weak interlayer bonding [1, 2]. More recently, research efforts have been directed toward optimizing and combining filament orientations to improve mechanical performance and thus optimize 3D-printing processes in terms of mechanical properties [6, 7]. Nevertheless, these works still mainly

address material-level issues, leaving out the problem of the performance of full prosthetic structures under realistic service conditions.

Furthermore, in addition to filament orientation, several printing process parameters, including layer thickness, print speed, and nozzle temperature, also influence the mechanical properties of the 3D-printed polymers. Thinner layers provide better interlayer bonding, whereas higher temperatures and optimized print speeds minimize the formation of cracks, warpage, and delamination defects [3, 4, 7, 8]. Although the above parameters have been extensively studied, their synergic effects on material properties and the interaction of filament orientation with the parameters have been insufficiently studied. As shown in the case of composite polymers, the combined effect of filament orientation and material composition is crucial for maximizing durability and mechanical characteristics [13–15]. In addition, most previous studies relied on standard tests with small samples to determine material properties. In turn, full prosthetic parts are expected to perform under various conditions that require the consideration of realistic loadings. During ambulation, for example, the structure of a prosthesis must withstand multiaxial, cyclic, and dynamic loads, thus requiring the consideration of realistic loading patterns. Ground reaction force (GRF) values can define loads applied to prosthetic shanks; however, GRF has seldom been used as a measurement in previous studies [16–20].

For this reason, an experimental-biomechanics-computational framework should be used to analyze the performance of additive manufacturing parts under realistic conditions. This study considers the effect of 3D printing orientation on the mechanical performance of prosthetic shanks. The study involved three different filament orientations and relied on tensile tests, fatigue tests, GRF data, and full-scale finite element analysis (FEA). In contrast to many previous papers, this work addresses a complete prosthetic structure instead of a certain material characteristic. By analyzing the effect of filament orientation on the stresses acting on a prosthetic shank and its mechanical performance, this study provides valuable information about a specific prosthesis rather than its material characteristics. Thus, this paper presents an advanced approach for assessing the performance of additive manufacturing prosthetic shanks based on experimental tensile and fatigue tests in combination with realistic biomechanical loading and FEA.

2 Material and Methods

2.1 Materials and Preparation of Specimens

Poly(lactic acid) (PLA) is one of the most researched biopolymer materials because of its special properties that distinguish it from other traditional petroleum-based thermoplastics, such as acrylonitrile-butadiene-styrene (ABS) and polyethylene terephthalate glycol (PETG). PLA is a biopolymer obtained from renewable sources, such as corn or sugarcane. PLA is fully biodegradable, which makes it extremely attractive with the shift towards a more sustainable future with green material approaches and green economic principles. PLA exhibits excellent dimensional stability and does not deform under loading. These are important properties for a material to be used for printing objects that must be structurally sound and dimensionally accurate. PLA has a density slightly higher than ABS (1.04 g/cm^3) and a density comparable to PETG (1.27 g/cm^3). PLA melts at a relatively low temperature of $150\text{--}160 \text{ }^\circ\text{C}$, which is substantially lower than the melting points of PETG ($230 \text{ }^\circ\text{C}$) and ABS ($210\text{--}250 \text{ }^\circ\text{C}$). This makes PLA easier to process with standard fused deposition modeling (FDM) machines without the need to heat the extruder to high temperatures or use a heated chamber. This reduces the energy required for the process and increases the reliability with which objects can be produced using PLA. PLA also has low thermal shrinkage when solidified, which minimizes the chances of errors with respect to accuracy, a problem that often occurs with ABS. PLA naturally has a smooth finish and shiny appearance, which are superior to those of ABS and PETG. These characteristics enable this material to be used in applications that require aesthetics.

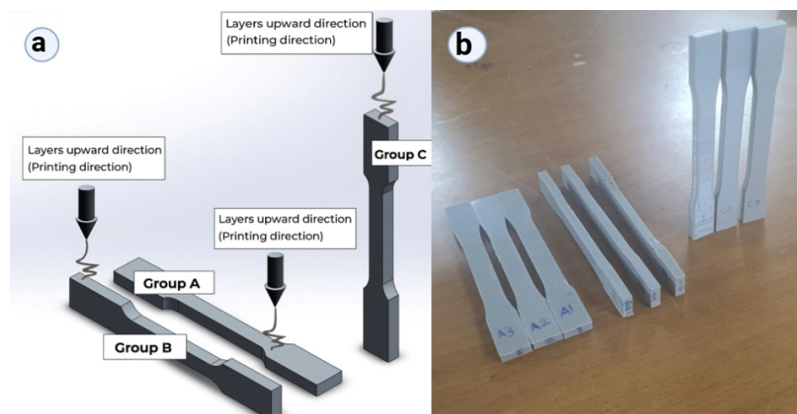


Figure 1. (a) Schematic of the tensile specimen; (b) printed tensile test specimens

Moreover, it generates a significantly lower number of harmful fumes during the extrusion process than ABS. This makes it a more convenient choice to work in a laboratory setting. The mechanical, physical, and environmental advantages of this material make it a prime choice for this research. This material was chosen as a reference material for this research because it provides a clear reference for isolating the effect of layer orientation. This material does not involve any complexity in terms of added fibers or other composite materials. This allows the effect of the mechanical aspects of printing orientation to be isolated before it is applied to more complex materials used in clinical applications. To enable better control of the printing orientation, all tensile test specimens were engineered using SolidWorks in accordance with American Society for Testing and Materials (ASTM) D638 standards [21]. Figure 1 presents three groups of tensile test specimens with varying orientations. The printing orientations were defined as follows: Orientation A corresponds to horizontal printing, where the filaments are aligned parallel to the loading direction; Orientation B represents an inclined configuration (approximately 45° relative to the loading direction), and Orientation C corresponds to vertical printing, where the layers are oriented perpendicular to the loading direction. An Anet ET4 FDM machine with a build area of 220 × 220 × 250 mm and a Cartesian motion system was used to carry out the additive manufacturing process. The machine is equipped with a nozzle diameter of 0.4 mm with a layer resolution ranging from 0.1 to 0.3 mm.

All settings for the 3D printing process used in this study were clearly spelled out to enable their repetition. The 3D printer used a 0.4 mm brass nozzle for fabrication. The extrusion temperature ranged from 200 to 205°C. The temperature of the heated bed was set to 60 °C. The outer edges were set to approximately 50 mm/s, while the infill was set to approximately 60 mm/s with a layer thickness of 0.20 mm. A rectilinear solid infill with 100% infill density was used to ensure that there were no empty spaces inside. The cooling fan was turned on after the first layer to ensure a stable extrusion. Ultimaker Cura 5.x with a standard PLA profile was used for slicing and generating the toolpath.

Support structures were used based on the orientation of the print. The horizontal print specimens (Group A and Group B) did not need any support, whereas the vertical print specimens (Group C) had few supports for stability at the lower overhang sections. These supports did not interfere with the gauge sections. To avoid thermal distortions and ensure that all the specimens were of the same size, the printing process took place in a controlled environment (23 ± 2 °C; 50 ± 5% RH).

This article clearly distinguishes between the full prosthetic shank and tensile specimens in terms of material properties. The shank simulation tests are for the performance of the device, whereas the specimen tests are for the material properties.

In addition to the static tensile properties, the fatigue properties of the printed specimens were considered based on the cyclic loading conditions to which the prosthetic components were subjected. Fatigue properties are critical for additively manufactured polymers, as the layered structure may affect crack propagation.

Although the main aim of this study was to investigate the effect of layer orientation on the tensile properties and structural performance, the fatigue properties were qualitatively addressed with respect to the anisotropic properties of the FDM process. Prosthetic shanks are subjected to millions of loading cycles during normal gait. Therefore, the fatigue properties of 3D printed PLA structures need to be understood to estimate their durability and avoid any possible failure.

Future work will involve conducting cyclic fatigue tests under specified stress conditions to simulate real-time loading conditions.

2.2 Design and Production of Prosthetic Shanks

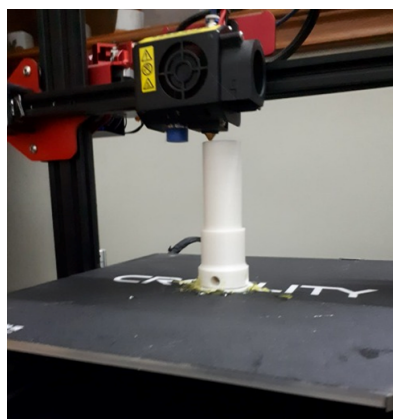


Figure 2. Fused deposition modeling (FDM) 3D printed prosthetic shank

To ensure proper fit and comfort, the prosthetic shank was measured anatomically and then modeled using SolidWorks. Design features for improved load, stability, and user mobility were incorporated into a computer-aided design (CAD) model. Once the model was completed, it was prepared for 3D printing by converting it to STL. As shown in Figure 2, a prosthetic shank was printed using PLA and a 3D printer.

2.3 Testing for Ground Reaction Force

The prosthetic shank interaction with the residual limb during the walking process can be quantitatively assessed by measuring the GRF. The subject of this study, as presented in the case study, was a 23-year-old female transtibial amputee with a total body weight of 50 kg. A three-axis force plate (AMTI OR6-7) with a capacity to measure 5 kN vertically, sensitivity of 2 mV/V, and sampling frequency of 1000 Hz was utilized to measure the GRF. The force plate can capture the subtle forces that occur during walking, such as heel strike and toe-off.

Before the tests were performed, the force plate was zeroed and calibrated. To observe natural walking behavior, several walking and running tests were performed by the participants at their own pace. Only those tests were taken into account in which the prosthetic foot came in complete contact with the plate were considered. The forces experienced by the prosthetic foot were revealed using a force plate.

GRF assessment is a well-established biomechanical assessment technique for evaluating prosthetic fit, prosthetic loading, gait, and possible discomfort or stress points [22]. The loading conditions used in the finite element simulation to improve prosthetic performance, structural reliability, and user comfort were derived from the results obtained from the measurement of the GRF.

3 Analysis of Numerical Data

SolidWorks Simulation 2023 software was used to carry out a full simulation to ascertain how this prosthetic shank would respond to a loading condition that simulated a walking scenario. The proximal interface of this prosthetic shank, where it connects to the knee adapter (Figure 3), was constrained in this simulation. This constraint represents a realistic fixation condition corresponding to prosthetic attachment during gait. This is an important constraint because it simulates a real-world constraint that would be observed in a prosthetic assembly in a walking scenario. The finite elements used in this simulation totaled 12,477 second-order tetrahedral elements (Figure 4). The mesh refinement feature was used in the distal and proximal regions to accurately capture the stress concentration zones. Mesh convergence analysis was performed until an iterative refinement resulted in a difference of less than 3% in the peak von Mises stress. The numerical analysis was derived from the equilibrium equation for linear elasticity, as follows:

$$\nabla \cdot \sigma + F = 0 \quad (1)$$

where, σ is the Cauchy stress tensor and F represents the external body forces. The analysis of the stresses was performed using the von Mises failure criterion, which is applicable in the evaluation of the multiaxial state of stress in the polymeric material of the FDM-processed parts.

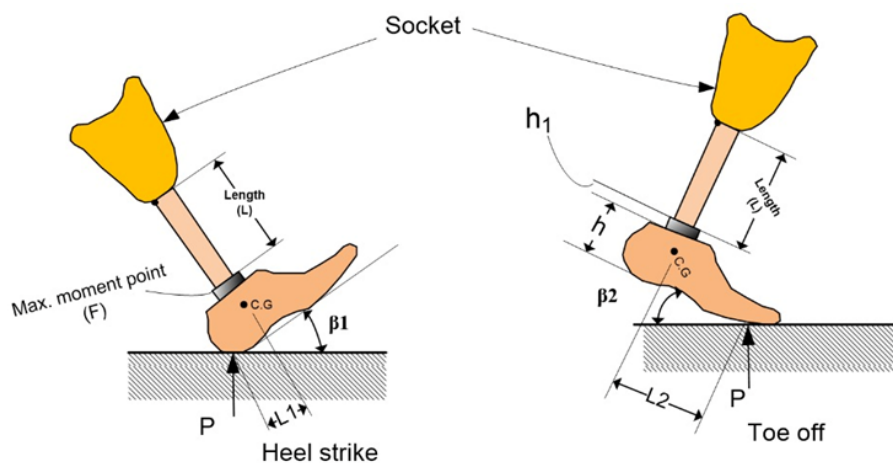


Figure 3. Heel strike and toe off forces distribution

For full conformity of the analytical expressions with the geometric representation in Figure 3, the symbols are unified throughout the text. The vertical dimension is referred to as $(h_1 + h)$, where L_1 and L_2 represent the horizontal offsets of heel strike and toe-off, respectively. The load angles are denoted as β_1 and β_2 , and the load

is denoted as P . These unified symbols are used throughout Section 3 and Figure 3 to prevent ambiguity in the interpretation of the model.

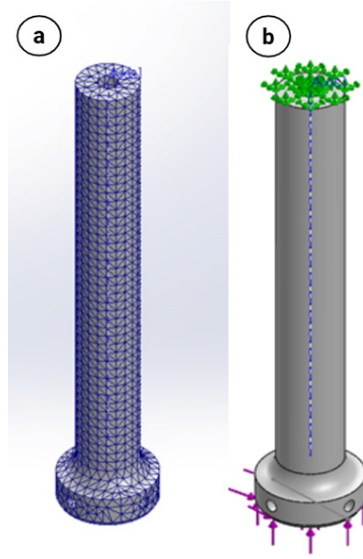


Figure 4. Finite element mesh and boundary loading configuration of the prosthetic shank: (a) mesh; (b) boundary conditions

The von Mises criterion was used to determine the stress, which is expressed as:

$$\sigma_{vm} = \sqrt{\left\{1/2 \left[(\sigma_x - \sigma_y)^2 + (\sigma_y - \sigma_z)^2 + (\sigma_z - \sigma_x)^2 \right] + 3 (\tau_{xy}^2 + \tau_{yz}^2 + \tau_{zx}^2) \right\}} \quad (2)$$

This is suitable for analyzing the behavior of polymeric materials under multiaxial conditions. A direct sparse solver is used because it is very good at dealing with static structural analysis problems that have complicated shapes.

The loads used in the simulation were based on GRF measurements conducted in the laboratory. These forces were transformed into equivalent bending moments and applied as distributed loads to accurately represent the physiological loading conditions during walking. In this case, the focus was on the heel-strike and toe-off phases of the gait cycle, as shown in Figure 3. At the critical point where the shank was at point F, the values of the GRF changed to bending moments that were the same. The bending moments used in the simulation were based on the following relationships:

At the heel strike:

To obtain a numerical solution, the moment below the shank must be determined and can be calculated as follows:

Moment at point F.

At heel strike:

$$M = P [\sin \beta_1 \cdot (h_1 + h) - \cos \beta_2 \cdot L_1] \quad (3)$$

At toe off:

$$M = P [\cos \beta_2 \cdot L_2 - \sin \beta_2 \cdot (h_1 + h)] \quad (4)$$

where, $(h_1 + h)$ is the vertical dimension, L_1 and L_2 are the corresponding horizontal distances, P is the applied ground reaction load, and β_1 and β_2 are the load angles at the heel strike and toe-off, respectively. To simulate realistic mechanical loading conditions in a biomechanical system, the analytically obtained results of the bending moments were applied as a distributed load along the proximal interface of the shank.

The FDM process resulted in geometric asymmetry that did not impose any symmetry conditions. The anisotropic effect of FDM printing on the deformation modes and stress distributions was substantial. Therefore, to consider this effect in the simulation model, the material input in the simulation model accounted for the nozzle movement direction in relation to the orientation of the printed layers. To ensure compatibility between the numerical results obtained from the simulation model and the tensile test results, the tensile properties obtained from the experiments were used as input in the simulation model. In the finite element model, anisotropic behavior was approximated using orientation-dependent material properties derived from tensile tests rather than implementing a fully orthotropic material model.

It was observed that there was a strong agreement between the stress concentrations obtained from the simulation model and the fracture modes obtained from experiments conducted on printed samples. This validates the simulation model. This shows that the structural response of the prosthetic shank to the walking conditions was accurately simulated in this numerical model.

4 Results and Discussion

4.1 Test of Tensile Strength

The yield stresses of the three groups of specimens manufactured with different printing orientations were found to vary based on the tensile test results, as shown in Table 1. The yield stress of Group C (24.7 MPa) exhibited a significant reduction, which corresponds to a reduction of approximately 60% compared with the horizontally printed specimens. Group A (61.3 MPa) exhibited the highest yield stress, followed by Group B (60.7 MPa). The modulus of elasticity values of all groups showed minimal variations between 1.480 and 1.523 GPa, indicating that the modulus of elasticity was not significantly affected by the orientation, unlike the tensile strength. The relatively low standard deviation values indicate good repeatability of the experimental results, despite the limited number of specimens.

Table 1. Results of tensile test

Group	Yield Stress (MPa)	Modulus of Elasticity (GPa)
A	61.3 ± 1.1	1.523 ± 0.015
B	60.7 ± 1.3	1.480 ± 0.018
C	24.7 ± 0.9	1.484 ± 0.016

Note: The reported values represent the mean ± standard deviation of the three specimens for each printing orientation.

To ensure that the results were statistically valid, the mechanical properties were reported as mean ± standard deviation based on three measurements from each printing orientation.

The above results validate the effect of the printing orientation on the tensile properties. Because the horizontal orientations of the printing process allowed for better interlayer fusion in the x - y plane, the mechanical properties were better. In the case of the vertical orientation, the interlayer bonding was poor along the z -axis, which reduced the mechanical properties. In the research conducted by Shah and Jain [1], they found that the PLA material had better tensile properties when printed horizontally compared to the vertical orientation. They explained that interlayer adhesion is better in the horizontal direction. Kaihara et al. [2] discussed the effect of the change in orientation on the mechanical properties of polymeric materials. They explained that the change in orientation directly affects the mechanical properties and stress distribution. Ewart [3] and Kasturi et al. [4] discussed the effect of printing direction on elasticity, fracture properties, and tensile properties. In the present study, yield stress showed significant variation with orientation, while the stiffness values were almost identical. In the research conducted by Helal et al. [9], they found that the interlayer bonding is poor along the z -axis, which reduces the mechanical properties. In the present study, vertically oriented samples exhibited poor performance. Tian et al. [10] pointed out that one of the major drawbacks of FDM-based biomedical devices is the interlayer weakness, particularly when subjected to multiaxial loading conditions. Furthermore, the research conducted by Pagáč et al. [11] discussed the anisotropic properties of the FDM process. They explained that the orientation of the printing process should be optimized. In the present study, the significant variation between the horizontally oriented samples and the vertically oriented samples was due to orientation. This behavior is directly attributed to the anisotropic nature of the FDM process, in which the interlayer bonding strength differs significantly depending on the loading direction relative to the filament orientation. This difference can be explained by the weak interlayer adhesion in the vertical orientation, where tensile loading promotes crack initiation and propagation along the layer interfaces, resulting in premature failure. It should be noted that these tensile results represent material-level behavior under uniaxial loading and will be further interpreted in relation to structural performance under bending conditions in subsequent sections. Aimar et al. [12] came to the same conclusion that the effect of the printing orientation should not be ignored while designing prosthetic components, as this may jeopardize the durability.

Overall, these results agree with the consensus in the literature that layer orientation is a crucial factor in determining tensile strength but does not significantly affect the modulus of elasticity of the material. The results obtained in this study provide proof of the importance of selecting a particular print trajectory in prosthetic applications, in addition to offering experimental evidence to support previous results. Following the suggestions of Ford and Despeisse [16] regarding orientation strategies for sustainable additive manufacturing, it is believed that orientations that allow for maximum bonding in the horizontal plane will ensure maximum reliability in terms of structures, particularly prosthetic shanks. Therefore, these results not only validate previous studies but also emphasize the importance of orientation selection in terms of its implications for prosthetic devices in satisfying

patients in terms of safety in the oral cavity. There were clear differences in the failure modes in terms of the orientation of the printed samples. The vertical samples exhibited clean brittle fractures, the horizontal samples exhibited clear interlayer delamination, and the diagonal samples exhibited mixed cracking modes. All these modes indicate that the FDM-printed PLA behaved in an anisotropic manner.

In addition to verifying the trends of anisotropy in FDM that have already been reported, the present study offers more information on the subject by correlating material properties with the performance of prosthetics on a full scale. The combined analysis of the tensile test, GRF, and stress distribution in the finite element model revealed that the relationship between the path of the filaments and the bending forces is more complex than that reported in previous studies. The shank does not fail because of the weak bonding between the layers but because of the increased stress caused by the moments generated by the act of walking, which worsens the mismatch in stiffness. This can be observed in the vertically oriented shanks, where the improved correlation between the path of the filaments and the bonding between the layers reduced stress peaks. The same can be seen in the horizontally oriented shanks, where bending increased the problems at the interfaces between the layers. Previous studies on this subject did not offer quantitative data, as they analyzed small samples taken from their environment. The present study offers more information on how orientation affects the durability of prosthetics, as it includes the forces of walking and stress flow due to failure, thus extending previous studies on this subject.

4.2 Fatigue Behavior of 3D Printed Prosthetic Components

Fatigue resistance is an important property of prosthetic components because they are always subjected to cyclic loading conditions in response to normal activities, such as walking and running. The fatigue response of the printed PLA samples was also investigated by studying the relationship between the stress amplitude and the number of cycles to failure using S–N curves, as depicted in Figure 5. The fatigue behavior presented in this study is based on controlled loading conditions; however, specific parameters, such as the stress ratio (R), loading frequency, and environmental conditions, were not standardized and are acknowledged as limitations of this study. The observed fatigue trends were consistent across the tested samples, indicating acceptable repeatability despite the limited number of specimens.

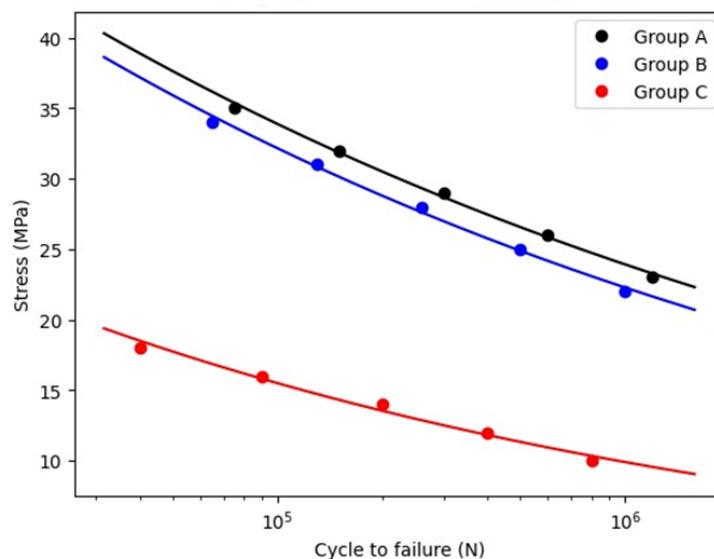


Figure 5. S–N fatigue curves of polylactic acid (PLA) specimens for three printing orientations (A, B, and C)

The results obtained indicate that fatigue life is dependent on the orientation of printing. The samples printed in orientation A exhibited the highest fatigue resistance. For instance, when the stress amplitude was 35 MPa, failure was observed after 7.5×10^4 cycles. However, when the stress amplitude was reduced to 23 MPa, the fatigue life was observed to increase to 1.2×10^6 cycles. The same trend was observed in the Group B samples. The samples had a fatigue life of 6.5×10^4 cycles when subjected to a stress amplitude of 34 MPa. However, the fatigue life was observed to increase to nearly 1.0×10^6 cycles when the stress amplitude was reduced to 22 MPa.

In contrast, the samples in Group C exhibited low fatigue resistance. For instance, when a stress amplitude of 18 MPa was used, failure was observed after 4.0×10^4 cycles. However, the fatigue life was observed to increase to 8.0×10^5 cycles when the stress amplitude was reduced to 10 MPa. This represents a significantly lower fatigue resistance compared to Groups A and B under similar loading conditions. This indicates that the fatigue life of Group C was

reduced by more than 40–50% compared to Groups A and B under comparable stress levels. The fatigue life of the samples in this group decreased in the following order: $A \approx B > C$.

This can be explained by the anisotropic properties of FDM. For the horizontally printed samples (Groups A and B), the filaments were oriented along the loading direction. Consequently, the load was transferred more efficiently, delaying the onset of cracks. For the vertically printed samples (Group C), the interfacial layers acted as the preferred sites for the initiation and propagation of cracks. From a fracture mechanics perspective, cyclic loading promotes crack initiation at weak interlayer boundaries, followed by progressive crack propagation, which significantly reduces the fatigue life of vertically printed specimens. These fatigue characteristics are consistent with the stress distribution patterns observed in the FEA, where regions of high stress concentration correspond to early crack initiation zones.

Similar trends were observed in the fatigue performance of additively manufactured polymers. Shah and Jain [1] observed that the fatigue durability of FDM-printed polymers is significantly affected by filament orientation. In this case, the samples printed along the loading direction exhibited improved fatigue durability. Similarly, Wickramasinghe et al. [13] observed that poor bonding between the layers is one of the primary factors that affect the fatigue performance of 3D printed polymer samples. As observed in the current study, printing orientation plays a significant role in improving the fatigue performance of prosthetic structures fabricated via additive manufacturing. It should also be noted that the presented S–N curves describe general fatigue trends, and future work will include standardized fatigue testing protocols and regression-based modeling for more accurate life prediction.

As observed in the current study, the fatigue strength decreased gradually with an increase in the number of cycles. This is a typical characteristic of polymeric materials subjected to fatigue loading. Therefore, printing orientation is essential for improving the durability of prosthetic structures fabricated via additive manufacturing.

4.3 Ground Reaction Force

GRF analysis is an established biomechanical tool that describes the interaction between prosthetic and residual limbs during walking. The design, optimization, and validation of prosthetic components are based on variations in the GRF during the gait cycle, thus providing better comfort, efficiency, and long-term structural reliability. Because these are the highest load values, they directly influence the mechanical requirements of the prosthetic shank. Importance was assigned to the heel strike and toe-off phases in this study.

A three-axis force plate (AMTI OR6-7, 5 kN vertical capacity, 2 mV/V sensitivity, and 1000 Hz sampling frequency) was employed to obtain the GRF data for the present study. Only data with complete prosthetic foot contact were included in the study, and participants walked at their own pace. Notably, the GRF data were obtained from a single-subject case study, which limits the generalizability of the results. These measurements were primarily used to provide representative loading conditions for FEA rather than to establish generalized biomechanical conclusions. The obtained values of the GRF showed a typical double-peaked pattern of human walking, as shown in Figure 6, where the second peak was high during the toe-off phase, and the initial peak was small during the heel-strike phase. The highest values of the GRF were observed during the toe-off phase. The peak GRF value approximately corresponded to the highest load applied to the prosthetic shank during gait. The peak load typically represents the maximum mechanical demand of the prosthetic shank during the gait cycle.

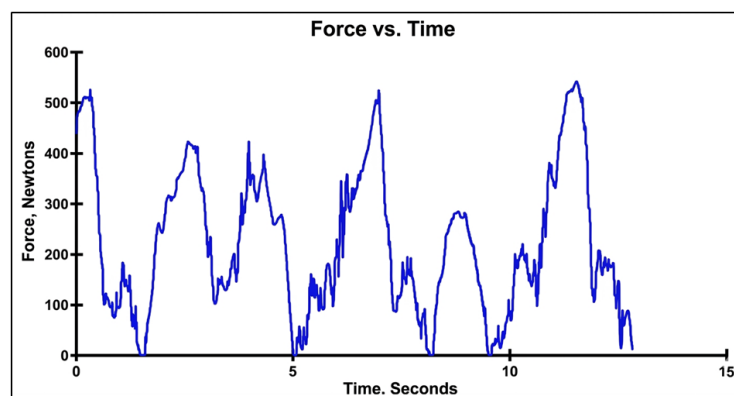


Figure 6. Ground reaction force (GRF) with gait cycle

The maximum value of the GRF, which occurred at toe-off, was selected as the input for the numerical simulation. Thus, it can be guaranteed that the FEA model experienced the most critical loading conditions. This approach ensures that the applied loading represents a conservative worst-case scenario for structural evaluation. Accordingly, these GRF values were directly implemented as boundary loading conditions in the finite element model to ensure a realistic simulation of the in-service behavior. Notably, this practice does not allow stress levels to be underestimated.

Additionally, it can be guaranteed that the evaluation of the prosthetic shank will include the worst-case conditions. It should be noted that this finding is consistent with the results of previous studies published in the literature. In this context, it should be noted that Tian et al. [10] emphasized the importance of validating prosthetic structures made of polymers with peak values of the GRF to guarantee the durability of prosthetic structures subjected to cyclic loading. Helal et al. [9] noted that prosthetic structures fabricated with additive manufacturing exhibited the highest levels of stress during the toe-off phase. In addition, it should be noted that according to the results of relevant studies in the field of biomechanics, the forces occurring during the heel-strike phase are lower than those occurring during the toe-off phase. In this context, it should be noted that this finding can be explained by the fact that the forces occurring during the double-peaked pattern are lower than those occurring during the toe-off phase [23].

Even under normal walking conditions, the variations in the GRF occurring during the gait cycle can be considered consistent with the prosthetic loading conditions. It should be noted that this practice can be used to demonstrate the limitations of assuming simplified loading conditions. In this context, it should be noted that Aimar et al. [12] emphasized that the evaluation of prosthetic structures should not ignore the gait cycle, as this may result in the underestimation of stress levels, which may cause early failure.

In conclusion, it can be noted that the results obtained in this study with respect to the GRF can be used to emphasize the importance of considering realistic loading conditions during the evaluation of 3D-printed prosthetic shanks. However, further studies involving multiple subjects are required to improve the statistical reliability and general applicability of GRF measurements. Therefore, the present findings should be interpreted as indicative rather than generalizable. It should be noted that this practice was supported in this context.

4.4 Analysis of Numerical Data

The results of the finite element simulations performed in SolidWorks provided more information on the effect of printing orientation on the structural performance of the prosthetic shank. In the present model, anisotropic behavior was approximated using orientation-dependent material properties derived from tensile tests rather than implementing a fully orthotropic material model. The vertically printed orientation offers the highest safety margin, implying that it has a greater ability to withstand the load transferred during walking. However, when the prosthetic shank was printed in the horizontal orientation, the safety margin significantly decreased, implying that it had a lower ability to withstand the load than the vertically printed orientation. This observation appears to differ from the tensile test results; however, this difference arises from the distinction between the material-level behavior and structural response under complex loading conditions.

The simulation results showed that the orientation of the filament in relation to the load plays a crucial role in determining the structural performance of the prosthetic shank. This trend can be explained by the anisotropic behavior of the FDM. A vertically printed orientation, in which the layers are perpendicular to the direction of the load, allows for better cohesion and load transfer. This orientation delayed the onset of failure and improved the resistance to deformation. However, interlayer adhesion becomes the dominant mode of failure when the layers are parallel to the load, as in the horizontal orientation, resulting in a decreased resistance. Under bending-dominated loading conditions, such as those induced by gait (GRF), the alignment of filaments relative to the principal stress directions becomes more critical than the uniaxial tensile strength measured at the material level. Similar results were reported by Shah and Jain [1] and Kaihara et al. [2], who found that printing PLA in the direction of the load decreased its tensile and flexural properties.

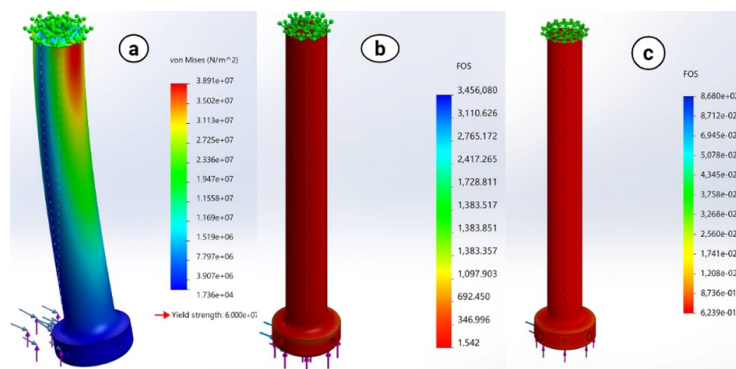


Figure 7. Numerical analysis: (a) Von Mises stress; (b) safety factor of case A; (c) safety factor of case B

Figure 7 illustrates the variations in the safety margins of the three printing orientations, confirming the inferiority of the horizontal orientation. This variation indicates a clear difference in structural performance, with the vertically printed configuration demonstrating a higher safety margin than the horizontal orientation. The results of Pagáč

et al. [11], in which the authors emphasized the susceptibility of parallel-layered FDM structures to early fracture and delamination, were consistent with the findings in the horizontally printed model. These results are consistent with the findings of Ewart [3], in which the authors emphasized the importance of mechanical anisotropy as one of the main concerns affecting the reliability of load-bearing biomedical components produced by the additive manufacturing process. The results of the present study are consistent with the findings of Aimar et al. [12] and Wickramasinghe et al. [13], who emphasized the importance of printing orientation in the long-term durability of structures.

The present study is an extension of previous research in this field in which the safety margin was simulated under gait-induced loading conditions. The results of the numerical simulations demonstrated the reliability of the vertical orientation of the prosthetic components. The numerical results were in good agreement with the GRF patterns described in Section 4.3. Furthermore, the apparent discrepancy with the tensile results was resolved by considering that the tensile tests represent uniaxial loading, whereas the prosthetic shank was subjected to multiaxial and bending stresses during walking. The numerical results are in good agreement with the tensile results in Section 4.1. The results of the numerical simulations showed that printing orientation plays an important role in the mechanical performance of prosthetic components.

Although statistical validation was not possible in this pilot-scale study, the FEA results showed good qualitative agreement with the experimentally observed failure modes and tensile results. The regions of maximum Von Mises stresses in the numerical results coincided with the regions where the specimens showed initial cracking or delamination. This confirms that failure is governed by stress concentration and interlayer weakness, which are strongly influenced by the filament orientation. This agreement further supports the validity of the simulation approach in capturing the anisotropic mechanical behavior of FDM-printed structures, despite the limited sample size. This simplified representation captures the dominant effect of filament orientation on mechanical behavior, although it does not fully account for complete orthotropic material coupling. However, it should be noted that the numerical results may be influenced by the modeling assumptions, boundary condition simplifications, and input variability, which represent inherent sources of uncertainty in FEA.

5 Conclusion

The results of this study showed that the mechanical properties of 3D-printed prosthetic shanks depend on the printing orientation. From the results of the tensile test, it was clear that the anisotropic behavior of the FDM printing technology was confirmed, where the horizontally printed specimens showed a higher yield strength (61.3 MPa) than the vertically printed specimens (24.7 MPa), representing a reduction of approximately 60%. The fatigue test results showed that the fatigue life of the 3D-printed prosthetic shanks also depended on the printing orientation. From the S–N curves, the fatigue life of the specimens printed in orientations A and B was higher than that of the specimens printed in orientation C. This is attributed to the poor interlayer bonding in the vertically printed structures, which causes cracks. The results of the GRF test showed that the toe-off phase is the loading condition that causes the highest load in the prosthetic shanks. From the results, the loading conditions were incorporated into the finite element model, indicating that the stress distribution and safety factor depend on the orientation of the layers. Despite the results of tensile testing, which showed better material properties for the horizontal orientation, FEA proved that using the vertical orientation offered a better safety factor under bending-dominated loads. It is evident that there needs to be differentiation between the two when considering the application, since structural behavior is not only influenced by material properties but also by load-filament alignment in real-life conditions. The uniqueness of this research was demonstrated by the fact that an integrated methodological framework was applied, which combined tensile and fatigue analyses of the material, along with biomechanical analysis of the forces and FEA of the entire prosthesis. However, it should be mentioned that the current research was based on limited specimen numbers and one participant in the study of GRF; therefore, the findings may only serve as indicative tendencies rather than absolute conclusions. Further research should be conducted with a greater number of samples and gait tests of multiple subjects.

Author Contributions

Conceptualization, Z.Y.H.; methodology, A.K.M. and D.A.A.; validation, K.K.R. and M.A.A.; formal analysis, A.K.M.; investigation, Z.Y.H. and M.A.A.; resources, K.K.R.; data curation, D.A.A.; writing—original draft preparation, Z.Y.H. and A.K.M.; writing—review and editing, A.M.F. and D.A.A.; visualization, M.A.A.; supervision, K.K.R., M.A.A., and A.M.F.; project administration, Z.Y.H. All authors have read and agreed to the published version of the manuscript.

Data Availability

The data used to support the findings of this study are available from the corresponding author upon request.

Acknowledgements

The authors sincerely thank the staff of Mustansiriyah University, Baghdad, Iraq, for their invaluable support and assistance during this project. Ongoing support and technical guidance are crucial for the successful conclusion of this study.

Conflicts of Interest

The authors declare that they have no conflict of interest.

References

- [1] A. K. Shah and A. Jain, "Physical, mechanical, and thermal characterization of unfilled and carbon fiber filled polyamide (PA) filaments and corresponding fused deposition modelling fabricated samples," in *Proceedings of International Manufacturing Science and Engineering Conference (MSEC 2024)*, Knoxville, Tennessee, USA, 2024, pp. MSEC2024–121 544, V001T02A001. <https://doi.org/10.1115/MSEC2024-121544>
- [2] F. H. Kaiahara, E. C. G. Pizi, F. G. Straioto, L. D. Galvani, M. C. Kuga, T. A. Arru e, and H. Vidotti, "Influence of printing orientation on the mechanical properties of provisional polymeric materials produced by 3D printing," *Polymers*, vol. 17, p. 265, 2025. <https://doi.org/10.3390/polym17030265>
- [3] P. Ewart, "A comparison of processing techniques for producing prototype injection moulding inserts," 2019. <http://researcharchive.wintec.ac.nz/id/eprint/7270>
- [4] S. Kasturi, A. N. Patil, P. Nandi, and N. Raikar, "Rapid prototyping assistance to medical science," *Int. J. Adv. Eng. Res. Sci.*, vol. 3, p. 236937, 2016. <https://doi.org/10.22161/ijaers/3.12.3>
- [5] P. Ewart, "Reducing risk in pre-production investigations through undergraduate engineering projects," 2019. <http://researcharchive.wintec.ac.nz/id/eprint/6998>
- [6] S. M. Lathers, "Fused filament fabrication of prosthetic components for trans-humeral upper limb prosthetics," phdthesis, Arizona State University, 2017. <https://core.ac.uk/download/pdf/132709607.pdf>
- [7] B. Landeen, "Design and validation of a multiple axis, passive 3D-printed ankle-foot prosthetic for functional gait," mastersthesis, University of South Dakota, 2025. <https://red.library.usd.edu/diss-thesis/337>
- [8] S. M. Abbas, K. K. Resan, M. A. Abdulrehman, and A. M. Flayyih, "Numerical and experimental investigation of mechanical performance, interface pressure distribution, and structural safety of glass fiber-reinforced below-knee prosthetic sockets," *ASEAN J. Sci. Technol. Dev.*, vol. 42, no. 3, p. 9, 2026.
- [9] M. A. Helal, A. Fadi-Alah, Y. M. Baraka, M. M. Gad, and A. N. M. Emam, "In-vitro comparative evaluation for the surface properties and impact strength of CAD/CAM milled, 3D printed, and polyamide denture base resins," *J. Int. Soc. Prev. Community Dent.*, vol. 12, p. 126, 2022. https://doi.org/10.4103/jispcd.JISPCD_293_21
- [10] Y. Tian, C. Chen, X. Xu, J. Wang, X. Hou, K. Li, and X. Lu, "A review of 3D printing in dentistry: Technologies, affecting factors, and applications," *Scanning*, vol. 2021, p. 1, 2021. <https://doi.org/10.1155/2021/9950131>
- [11] M. Pag ac, J. Hajny s, Q. P. Ma, L. Jan ar, J. Jan sa, P. Stefek, and J. M es icek, "A review of vat photopolymerization technology: Materials, applications, challenges, and future trends of 3D printing," *Polymers*, vol. 13, p. 598, 2021. <https://doi.org/10.3390/polym13040598>
- [12] A. Aimar, A. Palermo, and B. Innocenti, "The role of 3D printing in medical applications: A state of the art," *J. Healthc. Eng.*, vol. 2019, p. 5340616, 2019. <https://doi.org/10.1155/2019/5340616>
- [13] S. Wickramasinghe, T. Do, and P. Tran, "FDM-based 3D printing of polymer and associated composite: A review on mechanical properties, defects and treatments," *Polymers*, vol. 12, p. 1529, 2020. <https://doi.org/10.3390/polym12071529>
- [14] X. Kuang, D. J. Roach, J. Wu, C. M. Hamel, Z. Ding, T. Wang, and M. L. Dunn, "Advances in 4D printing: Materials and applications," *Adv. Funct. Mater.*, vol. 28, p. 1805290, 2018. <https://doi.org/10.1002/adfm.201805290>
- [15] L. G. Blok, M. L. Longana, H. Yu, and B. Woods, "An investigation into 3D printing of fibre reinforced thermoplastic composites," *Addit. Manuf.*, vol. 22, p. 176–186, 2018. <https://doi.org/10.1016/j.addma.2018.04.039>
- [16] S. Ford and M. Despeisse, "Additive manufacturing and sustainability: An exploratory study of the advantages and challenges," *J. Clean. Prod.*, vol. 137, p. 1573–1587, 2016. <https://doi.org/10.1016/j.jclepro.2016.04.150>
- [17] D. Kokkinis, M. Schaffner, and A. R. Studart, "Multimaterial magnetically assisted 3D printing of composite materials," *Nat. Commun.*, vol. 6, p. 8643, 2015. <https://doi.org/10.1038/ncomms9643>
- [18] T. J. Prater, Q. A. Bean, N. J. Werkheiser, M. M. Johnston, E. A. Ordonez, F. E. Ledbetter, and G. M. Nelson, "Summary report for the technical interchange meeting on development of baseline material properties and design guidelines for in-space manufacturing activities," 2016. <https://ntrs.nasa.gov/citations/20160006047>

- [19] F. Ciccone, A. Bacciaglia, and A. Ceruti, "Optimization with artificial intelligence in additive manufacturing: A systematic review," *J. Braz. Soc. Mech. Sci. Eng.*, vol. 45, p. 303, 2023. <https://doi.org/10.1007/s40430-023-04200-2>
- [20] E. A. Abbod, K. K. Resan, A. A. Salman, and M. A. Abdulrehman, "Development of a fail-safe protective adapter for osseointegrated prosthetic limbs: Experimental and numerical investigation," *Results Eng.*, vol. 28, p. 107403, 2025. <https://doi.org/10.1016/j.rineng.2025.107403>
- [21] ASTM International, "Standard test method for tensile properties of plastics (ASTM D638-14)," 2014. <https://store.astm.org/d0638-14.html>
- [22] A. S. Oliveira, C. I. Pircoveanu, and J. Rasmussen, "Predicting vertical ground reaction forces in running from the sound of footsteps," *Sensors*, vol. 22, p. 9640, 2022. <https://doi.org/10.3390/s22249640>
- [23] K. K. Resan, E. A. Abbod, and T. K. Al-Hamdi, "Prosthetic feet: A systematic review of types, design, and characteristics," *AIP Conf. Proc.*, vol. 2806, p. 060005, 2023. <https://doi.org/10.1063/5.0163345>

Nomenclature

σ	Cauchy stress tensor
F	External body forces
σ_{vm}	Von Mises equivalent stress
$\sigma_x, \sigma_y, \sigma_z$	Normal stress components in x, y, z directions
$\tau_{xy}, \tau_{yz}, \tau_{zx}$	Shear stress components
M	Bending moment at point F
P	Applied ground reaction load
h	Height component of the shank
h_1	Additional vertical dimensions of the shank
$(h_1 + h)$	Total vertical dimension
L_1	Horizontal offset distance at heel strike
L_2	Horizontal offset distance at toe-off
Greek symbols	
σ	Normal stress/Cauchy stress tensor
τ	Shear stress
β_1	Load angle at heel strike
β_2	Load angle at toe-off
Subscripts	
vm	Von Mises
x, y, z	Cartesian coordinate directions
xy, yz, zx	Shear plane directions
1	Heel strike phase
2	Toe-off phase